

Theory of relativistic cyclotron masers

G. S. Nusinovich and P. E. Latham

Institute for Plasma Research, University of Maryland, College Park, Maryland 20742

O. Dumbrajs

Nuclear Engineering Laboratory, Helsinki University of Technology, SF-02150 Espoo, Finland

(Received 24 January 1995)

In this paper we have made an attempt to review the present status of the theory of cyclotron masers with relativistic electron beams. After discussing the basic features of electron-cyclotron radiation under conditions of normal and anomalous Doppler frequency shifts, we consider particle deceleration by a constant amplitude electromagnetic wave in a constant magnetic field using the formalism developed earlier for cyclotron autoresonance acceleration of electrons. An optimal cyclotron resonance mismatch was found that corresponds to the possibility of complete deceleration of relativistic electrons. Then, interaction of relativistic electrons with resonator fields is considered and the efficiency increase due to electron prebunching is demonstrated in a simple model. Since an efficient interaction of relativistic electrons with the large amplitude electromagnetic field of a resonator occurs at a short distance, where electrons make a small number of electron orbits, the issue of the simultaneous interaction of electrons with the field at several cyclotron harmonics is discussed. Finally, we consider deceleration of a prebunched electron beam by a traveling electromagnetic wave in a tapered magnetic field. This simple modeling is illustrated with a number of simulations of relativistic gyrokylystrons and gyrotwistrons (gyrodevices in which the bunching cavity of the gyrokylystron is combined with the output waveguide of the gyro-traveling-wave-tube).

PACS number(s): 52.75.Ms, 41.60.Cr

I. INTRODUCTION

The history of cyclotron masers began in the late 1950s when the first papers by Twiss [1], Schneider [2], Pantell [3], and Gaponov [4] were published, practically simultaneously and, obviously, independently (see also [5]). In these papers it was shown that electron beams moving in a homogeneous external magnetic field are capable of producing coherent bremsstrahlung radiation due to the relativistic dependence of the electron-cyclotron frequency on the electron energy.

The surprising peculiarity of these studies was the fact that the relativistic dependence played a crucial role even in the case of weakly relativistic electron beams. In such a case the interaction space must be long enough for the electrons to develop orbital bunching from the weak initial modulation in electron-cyclotron frequencies.

Gaponov considered the situation in a more general manner by also taking into account the effect of electron bunching caused by the axial inhomogeneity of the amplitude of the electromagnetic (em) wave. (This bunching, related to the Weibel instability [6], can also be considered as the result of changes in electron axial momentum under the action of the transverse component of the magnetic field of the wave.) Gaponov studied the simultaneous effect of the orbital bunching caused by the relativistic dependence of the electron-cyclotron frequency on electron energy and the axial bunching caused by changes in electron axial momentum. He found that when the em wave propagates along an external magnetic field at the speed of light, these two bunching effects completely compensate each other [7] (see also [8,9]). A similar analysis of the motion of a single electron in a con-

stant external magnetic field and a circularly polarized constant amplitude em wave propagating along the magnetic field led Kolomenskii and Lebedev [10] and Davydovsky [11] to the concept of autoresonance, in which an electron, initially in exact cyclotron resonance with the em wave, maintains this resonance even as its energy changes by arbitrarily large amounts.

The first half of the 1960s was a time of active study of cyclotron masers in different countries (see review papers [5,12]). Especially successful were the studies done at the Radiophysical Research Institute (Gorky, Soviet Union) where Gaponov and co-workers invented in 1966 a practical configuration of a cyclotron maser, the gyrotron [13,14]. During the second half of the 1960s and the first half of the 1970s gyrotrons became the most powerful sources of coherent millimeter- and submillimeter-wave radiation. These devices were capable of operating in the cw regime, and were successfully used in plasma experiments for electron-cyclotron plasma heating in tokamaks [15] (see also [12,16]). These successes led to the recognition of gyrotrons throughout the world and initiated gyrotron development in many countries, starting in the second half of the 1970s.

At present the theory of cyclotron resonance masers with weakly relativistic electron beams (including conventional gyrotrons) is well developed. In its general form this theory is based on the assumption that electrons gyrating in an external magnetic field interact with the em field under conditions of cyclotron resonance,

$$\omega - k_z v_z \approx s \Omega_c , \quad (1)$$

and make a large number of electron orbits in the interaction space, i.e.,

$$N = \frac{\Omega_c T}{2\pi} \gg 1 . \quad (2)$$

In Eqs. (1) and (2) ω and k_z are the frequency and axial wave number of the em wave, respectively, Ω_c and v_z are the relativistic electron-cyclotron frequency and electron axial velocity, respectively, s is the resonant harmonic number, and $T=L/v_z$ is the time of transit through the interaction region of length L . The term "weakly relativistic electron beams" used above implies that the electron kinetic energy is much smaller than the rest energy.

According to the conditions given by Eqs. (1) and (2), one can average the equations for the electron motion over the fast gyration. This results in a set of normalized equations which includes only the harmonic of the electromagnetic field rotating synchronously with the gyrating electrons. These slow time scale equations can be studied once and the results applied to an arbitrary mode and set of beam parameters (see, e.g., [14,16,17] and references therein).

The theory of cyclotron masers with relativistic electron beams is more complicated because of the strong relativistic dependence of the electron-cyclotron frequency on the electron energy. To explain this statement let us consider for simplicity gyrotrons operating in a uniform magnetic field $B_0\hat{z}$ at frequencies near the cutoff frequency of the resonant structure [in this case the axial wave number k_z in Eq. (1) is much smaller than ω/c].

When electrons change their energy \mathcal{E} in the process of interaction with the em field one can present the deviation in electron-cyclotron frequency $\Omega_c = eB_0/m_0c\gamma$ caused by the change in normalized energy, $\gamma = \mathcal{E}/m_0c^2$, as

$$\frac{\Delta\Omega_c}{\Omega_{c0}} = -\frac{\Delta\gamma}{\gamma_0} . \quad (3)$$

Here, $\gamma_0 = 1 + eV_b/m_0c^2$ is the initial value of γ and V_b is the beam voltage. Correspondingly, introducing the transit angle of electrons as the value proportional to the cyclotron resonance mismatch, $\Theta = (\omega - s\Omega_c)T$ (we omitted here the Doppler term, which is small in gyrotrons), one can find that the change in electron energy $\Delta\gamma$ causes a shift in the transit angle

$$\Delta\Theta = s\frac{\Delta\gamma}{\gamma_0}\Omega_{c0}T . \quad (4)$$

To change the electron energy without disturbing the cyclotron resonance, we must have $|\Delta\Theta| \lesssim 2\pi$ [14,18], which implies that

$$\frac{\Delta\gamma}{\gamma_0} \lesssim \frac{1}{sN} . \quad (5)$$

For efficient operation, in which all of the electron kinetic energy is withdrawn by the em field, the change in γ is $\Delta\gamma \sim eV_b/m_0c^2$, and the number of electron orbits must satisfy the condition

$$N \lesssim \frac{1}{s} \frac{m_0\gamma_0c^2}{eV_b} = \frac{1}{s} \frac{\gamma_0}{\gamma_0 - 1} . \quad (6)$$

There are a number of implications of Eq. (6). One of the most immediate is that relativistic gyrotrons with $|\gamma_0 - 1| \gtrsim 1$, for which the right hand side is of order 1, cannot operate efficiently in the same regime as their non-relativistic counterparts (close to cutoff with a large number of cyclotron orbits). One can, of course, operate with a short cavity (where the number of cyclotron orbits is small) and a constant magnetic field. One disadvantage of this approach is that to decelerate relativistic electrons in a short distance a large electric field is required, which may lead to microwave breakdown. A second problem arises because when $N \sim 1$ the device loses its resonant properties since the width of the cyclotron resonance band is on the order of the cyclotron frequency. Therefore the simultaneous excitation of several modes in such a wide band may occur. (Note that in relativistic gyrotrons TM modes can be competitive [17] with TE modes widely used in conventional gyrodevices.) In addition, the overlapping of cyclotron resonances at different harmonics becomes possible. So, while mode competition can be avoided to some extent by operating at low order modes, the harmonics overlapping at $N \sim 1$ looks unavoidable. Besides a complication of the theory describing the interaction, this can lead to degradation of the electron efficiency as will be shown below. This approach does have an advantage, however: it is relatively insensitive to the spread in electron energies and velocities.

The requirement that the electrons execute a small number of orbits can be relaxed if we allow Doppler up-shifted operation and a nonuniform magnetic field. When these effects are included, the expression for the transit angle is $\Theta = (\omega - s\Omega_c - k_z v_z)T$ and Eq. (4) for the change in transit angles becomes

$$\Delta\Theta = 2\pi sN \left[\frac{\Delta\gamma}{\gamma_0} - \frac{k_z v_{z0}}{s\Omega_{c0}} \frac{\Delta v_z}{v_{z0}} - \frac{\Delta B_0}{B_0} \right] . \quad (7)$$

Thus there are two strategies for ensuring that $\Delta\Theta \leq 2\pi$ while retaining a large number of cyclotron orbits. The first strategy is to choose the axial wave number k_z large enough so that changes in axial velocity partially compensate for changes in energy; i.e., the second term on the right hand side of Eq. (7) partially cancels the first. As was mentioned above, when $k_z = \omega/c$ this cancellation is complete and there is an exact autoresonance between electrons and the em wave. That is why cyclotron masers based on the effect of partial compensation of the first two terms in Eq. (7) are called cyclotron autoresonance masers, or CARMs. (CARMs were suggested by Petelin in 1974 [19]. The first review of theoretical studies of CARMs was done in 1981 [20]. The most recent reviews are given in Refs. [21,22].) Note that the em field excited in a short resonator can also be represented as a superposition of waves with rather large k_z . This issue will be discussed below.

The second strategy is to profile the external magnetic field so it matches the axial dependence of the energy of decelerating electrons [last term in Eq. (7)]. In such a case the cyclotron frequency of at least one synchronous electron remains constant so that cyclotron resonance between the em wave and this particle is maintained. For

other electrons there is a spread in cyclotron frequencies caused by different axial dependencies of electron energies that degrades the total efficiency of the electron beam deceleration. This method has been studied in relativistic gyrotrons and cyclotron masers with traveling waves, respectively, in [23] and [24] (see also [25]).

The above strategies may lead to high efficiency when idealized electron beams (with no velocity spread) are considered. However, the efficiency of these two kinds of operation can be sensitive to electron velocity spread. Therefore, to achieve high efficiency with relativistic electron beams it may be necessary to combine all three methods; i.e., provide a short interaction region, taper the external magnetic field, $B_0(z)$, and have the em waves propagate along the magnetic field with a finite axial wave number [26]. Of course, the corresponding optimization of parameters is a very complicated numerical problem, especially for gyroamplifiers: the search for optimal parameters takes place in the function space of axial magnetic field distributions and cavity shapes as well as the multidimensional parameter space of pitch ratio, input power, beam placement, and drift section length [27]. The equations that have to be studied in this case consist of the nonaverage equations of electron motion and the equations describing the spatial structure and the amplitude of the em field in the microwave circuit [28,29]. To facilitate such a search and to elucidate the results, it is expedient to consider the problem, first, in a simplified analytical manner, and then to approach the real situation by adding to the analysis successively the factors important for operation of realistic gyrodevices.

This paper takes just such an approach. First, in Sec. II we consider deceleration of one relativistic electron gyrating in a constant external magnetic field and interacting with a circularly polarized plane em wave. We then analyze the effect of an electron distribution in initial gyrophases on the efficiency of interaction. In Sec. III we study the same effect in the resonators where electrons excite standing waves. In Sec. IV we discuss the effect of overlapping of cyclotron resonances which may occur in strong fields excited in short cavities. Section V is devoted to the opposite case, i.e., the gradual deceleration of electrons in a tapered magnetic field in the process of interaction with the traveling wave. Finally, in Sec. VI we summarize our results.

II. INTERACTION OF GYRATING ELECTRONS WITH ELECTROMAGNETIC WAVES

Let us start by considering electrons moving in a constant external magnetic field B_0 and interacting with an electromagnetic wave. The electron motion can be described by the equations for the electron momentum,

$$\frac{d\mathbf{p}}{dt} = -e \left\{ \mathbf{E} + \frac{1}{c} [\mathbf{v} \times (\mathbf{B}_0 + \mathbf{B})] \right\} \quad (8)$$

and energy

$$\frac{d\gamma}{dt} = -\frac{e}{m_0 c^2} (\mathbf{v} \cdot \mathbf{E}) . \quad (9)$$

Here γ is the electron energy normalized to the rest energy $m_0 c^2$. In principle Eq. (9) is redundant since it can be derived from Eq. (8), but it is sometimes convenient to have an equation that tells us directly how the energy evolves.

For simplicity, let us consider a circularly polarized, constant amplitude, plane homogeneous transverse electromagnetic (TEM) wave propagating along \mathbf{B}_0 with the phase velocity v_{ph} that corresponds to its propagation in a medium with the refractive index $n = c/v_{ph}$. The vector potential of such a wave, $\mathbf{A} = A_x \mathbf{x}_0 + A_y \mathbf{y}_0$, can be presented in a complex form

$$A_x + i A_y = A e^{i(\omega t - k_z z)} , \quad (10)$$

where the axial wave number k_z is related to v_{ph} as $k_z = \omega/v_{ph}$ and A is the complex wave amplitude. Correspondingly, transverse components of the electron momentum can be presented in a complex form as $p_x + i p_y = p_\perp e^{i\theta}$ where θ is the electron gyrophase. Then, one can express the electric and magnetic fields of the wave via the vector potential \mathbf{A} by

$$\mathbf{E} = -\frac{1}{c} \frac{\partial \mathbf{A}}{\partial t}, \quad \mathbf{B} = \text{rot } \mathbf{A}$$

and rewrite Eqs. (8) and (9) as (cf. [19,20])

$$\frac{dp_\perp}{d\xi} = -\frac{\gamma - np_z}{p_z} \text{Im}(A e^{i\varphi}) , \quad (11a)$$

$$\frac{d\varphi}{d\xi} = \frac{\gamma}{p_z} \left[\frac{\omega - k_z v_z - \Omega_c}{\omega} - \frac{\gamma - np_z}{\gamma p_\perp} \text{Re}(A e^{i\varphi}) \right] , \quad (11b)$$

$$\frac{dp_z}{d\xi} = -n \frac{p_\perp}{p_z} \text{Im}(A e^{i\varphi}) , \quad (11c)$$

$$\frac{d\gamma}{d\xi} = -\frac{p_\perp}{p_z} \text{Im}(A e^{i\varphi}) . \quad (11d)$$

Here, time is presented as $t = t_0 + \tau$ where t_0 is the entrance time, τ is related to z as $dz/d\tau = v_z$, $\varphi = \omega t - k_z z - \theta$ is the phase of the wave with respect to the electron gyrophase, the electron velocity components are normalized to the speed of light, c , the electron momentum components to $m_0 c$, the wave amplitude A to $m_0 c^2/e$, and ξ to the axial coordinate, $\xi = \omega z/c$. Combining Eqs. (11c) and (11d) gives us the autoresonance integral derived in Refs. [10] and [11]:

$$n\gamma - p_z = n\gamma_0 - p_{z0} . \quad (12)$$

As follows from Eq. (12), decelerating electrons lose their axial momentum when they interact with the forward wave ($v_{ph} > 0$, and hence $n > 0$) and gain it when they interact with the oppositely propagating wave ($v_{ph} < 0$, $n < 0$). In the latter case the electron energy is withdrawn only from the orbital gyration of particles.

Combining Eq. (12) with the general relation between electron energy and momentum

$$\gamma^2 = 1 + p_\perp^2 + p_z^2 \quad (13)$$

one can determine the squared orbital momentum of electrons:

$$p_1^2 = p_{10}^2 - 2(1-n\beta_{z0})\gamma_0(\gamma_0 - \gamma) + (1-n^2)\gamma_0 - \gamma)^2. \quad (14)$$

From Eqs. (12) and (14) one can find for arbitrary values of the initial electron energy, γ_0 , and pitch ratio, $\alpha_0 = \beta_{10}/\beta_{z0}$, the optimal phase velocity of the wave [30] normalized to c :

$$\beta_{ph, opt} = \left[\frac{(1+\alpha_0^2)(\gamma_0 - 1)}{\gamma_0 + 1} \right]^{1/2}. \quad (15)$$

When $\beta_{ph} = \beta_{ph, opt}$ the electrons can be completely decelerated by the wave. When $\beta_{ph} > \beta_{ph, opt}$, electrons lose all their orbital momentum when the axial momentum is still finite. In the opposite regime, $\beta_{ph} < \beta_{ph, opt}$, the electrons lose all their axial momentum before the orbital momentum goes to zero, resulting in reflection of the particles.

Since a spread in electron axial velocities is inherent in electron beams, to avoid the appearance of reflected particles one should operate with $\beta_{ph} > \beta_{ph, opt}$. In such a case, when electrons lose all their orbital momentum the efficiency of kinetic energy extraction from one particle [single-particle efficiency, $\eta_{SP} = (\gamma_0 - \gamma)/(\gamma_0 - 1)$], as follows from Eq. (14), is equal to

$$\eta_{SP} = \frac{1}{1 - \gamma_0^{-1}} \frac{1 - n\beta_{z0}}{1 - n^2} \left\{ 1 - \left[1 - \beta_{10}^2 \frac{1 - n^2}{(1 - n\beta_{z0})^2} \right]^{1/2} \right\}. \quad (16)$$

When the last term in this expression is small,

$$\beta_{10}^2 \ll \frac{(1 - n\beta_{z0})^2}{|1 - n^2|}, \quad (17)$$

Eq. (16) is reduced to the known result [20]

$$\eta_{SP} = \frac{\beta_{10}^2}{2(1 - \gamma_0^{-1})(1 - n\beta_{z0})}. \quad (18)$$

For "gyrotron" operation at frequencies near cutoff ($n \ll 1$) Eq. (17) means weakly relativistic orbital velocities of electrons: $\beta_{10}^2 \ll 1$.

It follows from Eq. (15) that the interaction of electrons with fast waves ($\beta_{ph} > 1$) is optimal only at large enough pitch factors, i.e., when $\alpha_0^2 \geq 2/(\gamma_0 - 1)$. For intermediate values of α_0 [$1/\gamma_0 \leq \alpha_0^2 \leq 2/(\gamma_0 - 1)$] the optimal phase velocity corresponds to the interaction of electrons with slow waves ($\beta_{ph} < 1$) under the condition of the normal Doppler effect, $\beta_{z0} < \beta_{ph}$. Finally, for small α_0 ($\alpha_0^2 < 1/\gamma_0$) it is necessary to slow down the phase velocity of the wave even more and, therefore, the optimal phase velocity corresponds to the slow-wave interaction when the anomalous Doppler effect, $\beta_{z0} > \beta_{ph}$, takes place. Note that when electrons interact with the forward wave under the condition of the normal Doppler effect, they simultaneously lose both orbital and axial components of their momentum. However, under the condition of anomalous Doppler effect the electrons start their deceleration by losing axial and gaining orbital momentum [31]. In such a case one can use initially

linear electron beams (with $\beta_{10} = 0$) for coherent cyclotron radiation [19,32]. (Such beams can be formed more easily and of higher quality than beams moving along helical trajectories.) The physics of such a slow-wave cyclotron maser operating under the condition of the anomalous Doppler effect was considered in Refs. [33–35]. Note that in the process of deceleration under the condition of anomalous Doppler effect the electrons lose their axial momentum, so their axial velocity moves to the border between anomalous and normal Doppler effects, $\beta_z = \beta_{ph}$. An electron reaches this border when its energy change is equal to [33]

$$\gamma_0 - \gamma = \frac{\beta_{z0}\beta_{ph}^{-1} - 1}{\beta_{ph}^{-2} - 1} \gamma_0. \quad (19)$$

In the process of further deceleration the electrons lose both components of their momentum and, according to Eqs. (12)–(14), can be completely decelerated.

Note that Eqs. (11a)–(11d) contain one more integral. To derive it let us multiply Eq. (11a) by $(d\varphi/d\xi)$ and Eq. (11b) by $dp_\perp/d\xi$ and equate the right-hand sides of the resulting expressions. Then, using Eqs. (12) and (14), we can derive the equation

$$\frac{\Omega_{c0}\gamma_0}{\omega} \frac{d\gamma}{d\xi} = \frac{1}{2} \frac{dp_\perp^2}{d\xi} - \text{Re} \left[A \frac{d}{d\xi} (p_\perp e^{i\varphi}) \right]. \quad (20)$$

For the case of the constant wave amplitude and external magnetic field this gives us the following integral (cf. [36]):

$$\frac{\Omega_{c0}\gamma_0}{\omega} \gamma - \frac{p_\perp^2}{2} + \text{Re}(Ap_\perp e^{i\varphi}) = \text{const}. \quad (21)$$

This equation shows us how the phase φ varies with changes in electron energy and orbital momentum.

Both the autoresonance integral, Eq. (12), and the above conservation law, Eq. (21), have a quantum mechanical interpretation. This can be understood by observing that particles change energy and momentum by absorbing or emitting photons. In each elementary act of photon radiation or absorption for an electron energy change of $\hbar\omega$, the axial momentum changes by $\hbar k_z$; thus the factor of n in Eq. (13) [19]. The corresponding change in canonical angular momentum is \hbar , which, after some algebra, leads to Eq. (21). Note that the quantity $p_\perp^2/2 - \text{Re}(Ap_\perp e^{i\varphi})$ is proportional to the canonical angular momentum around a guiding center of a gyrating electron through first order in the vector potential \mathbf{A} .

Using Eqs. (12), (14), and (21), one can reduce the set of Eqs. (11a)–(11d) to one equation for the electron energy. This was done by Roberts and Buchsbaum in Ref. [37]. In our notations this equation can be written in the form

$$\beta_z^2 \left[\frac{d\gamma}{d\xi} \right]^2 = -V(\gamma), \quad (22)$$

where the function $V(\gamma)$ describing an effective potential well is equal to

$$V = \frac{1}{4\gamma^2} \mathcal{J}(\gamma),$$

and, as follows from Eqs. (12) and (15), for optimal n , $\beta_z\gamma=n(\gamma-1)$. Here \mathcal{J} is a fourth order polynomial of γ with coefficients depending on the initial electron energy, γ_0 , pitch ratio, α_0 , normalized wave amplitude, $a=(\Omega_{c0}/\omega)(E/B_0)$ (where E is the amplitude of the electric field of the wave), initial cyclotron resonance mismatch, $\delta=1-n\beta_{z0}-\Omega_{c0}/\omega$, wave phase velocity, β_{ph} (refractive index n), and entrance phase, φ_0 :

$$\begin{aligned}\mathcal{J} = & C_1(\gamma - \gamma_0)^4 + C_2\gamma_0(\gamma - \gamma_0)^3 + C_3\gamma_0^2(\gamma - \gamma_0)^2 \\ & + C_4\gamma_0^3(\gamma - \gamma_0) + C_5\gamma_0^4,\end{aligned}\quad (23)$$

with

$$\begin{aligned}C_1 &= (1-n^2)^2, \\ C_2 &= 4\delta(1-n^2), \\ C_3 &= 4[\delta^2 + (1-n^2)a(\beta_{10}\cos\varphi_0 - a)], \\ C_4 &= 8\delta a \beta_{10} \cos\varphi_0 - 8a^2(1-n\beta_{z0}), \\ C_5 &= -4a^2 \beta_{10}^2 \sin^2\varphi_0.\end{aligned}$$

Analyzing this function, $\mathcal{J}(\gamma)$, for the case of the optimal refractive index defined by Eq. (15) as $n_{opt}=\beta_{ph, opt}^{-1}$, one can find the optimal cyclotron resonance mismatch,

$$\delta_{opt} = \frac{\gamma_0}{\gamma_0-1}\beta_{10}a \cos\varphi_0 + \frac{\gamma_0-1}{2\gamma_0}(1-n_{opt}^2), \quad (24)$$

which depends only on three parameters: γ_0 , α_0 , and $a \cos\varphi_0$. Two terms on the right-hand side of Eq. (24) show that the cyclotron resonance mismatch must be chosen to account for both the wave amplitude (first term) and the departure from autoresonance (second term). Equation (24) follows from the equation $\mathcal{J}=0$ for $\gamma=1$, which means complete deceleration of a particle. For $\delta \neq \delta_{opt}$, $\mathcal{J}(\gamma=1)$ is positive, which means that electrons cannot be decelerated completely. Of course, it is impossible to provide simultaneously the optimal mismatch for electrons differing in entrance phases.

As was pointed out in [36–38], Eq. (22) as well as Eqs. (11a)–(11d) admit a general solution in terms of Weierstrassian elliptic functions. However, this formulation is not very useful. To obtain concrete results it is simpler to just integrate Eq. (22) numerically. Such an integration was done by the authors of [37] who considered, following [10] and [11], the case of exact initial cyclotron resonance, $\delta=0$, since they were interested in cyclotron autoresonance acceleration of charged particles. We mention also Ref. [39] where this formalism was used for describing cyclotron masers operating under anomalous Doppler conditions, and Ref. [40] where electron deceleration in the case of exact autoresonance ($n=1$) has been studied.

However, for deceleration of relativistic electrons by an electromagnetic wave, as follows from Eqs. (15) and (24), the case of nonzero cyclotron resonance mismatch and departure from exact autoresonance is of interest. Therefore we studied Eq. (22) for nonzero cyclotron resonance mismatch and the phase velocity of the wave different from the speed of light.

We started our study from analyses of the function

$\mathcal{J}(\gamma)$ defined by Eq. (23). Our results are illustrated in Fig. 1, where the potential well described by the function $\mathcal{J}(\gamma)$ is shown for optimal and nonoptimal values of the refractive index n and the cyclotron resonance mismatch δ . Figure 1(a) corresponds to a small wave amplitude ($a=0.02$) and Fig. 1(b) to a large one ($a=0.2$). These figures are given for initial normalized energy $\gamma_0=2$ and pitch angle $\alpha_0=1.5$. When both n and δ are optimal, $\mathcal{J}(\gamma)=0$ when $\gamma=1$; that which means a possibility of complete deceleration of particles.

From the curves $\mathcal{J}(\gamma)$ shown in Fig. 1 one can easily estimate the sensitivity of a single-particle efficiency to small changes in the parameters. The single-particle efficiency can be defined as $\eta_{SP}=(\gamma_0-\gamma_f)/(\gamma_0-1)$ where the final energy, γ_f , is defined as a root of the equation $\mathcal{J}(\gamma_f)=0$. In particular, one can find from such figures that the interaction efficiency becomes sensitive to

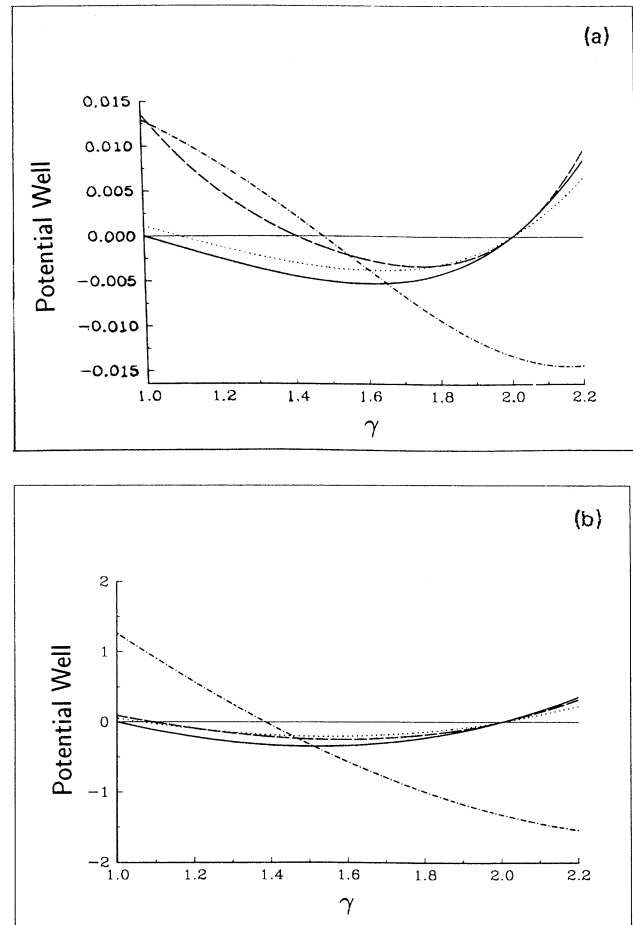


FIG. 1. Potential well in the cases of small (a) and large (b) wave amplitudes: solid lines correspond to $\varphi_0=0$ and optimal values of the refractive index, n , and the cyclotron resonance mismatch, δ ; dashed lines correspond to $n=0.9$ instead of $n_{opt}=0.96$ (other parameters are the same as for solid lines); dash-dotted lines correspond to $\varphi_0=\pi/4$ (other parameters are the same as for solid lines); dotted lines correspond to $\delta=0.04$ instead of $\delta_{opt}=0.048$ (a) and $\delta=0.25$ instead of $\delta_{opt}=0.3$ (b) (other parameters are the same as for solid lines).

the spread in initial gyrophases when it is on the order of $\pi/2$ or larger. It is also interesting to note that the same deviation of the refractive index from its optimal value determined by Eq. (15) causes large changes in efficiency when the wave amplitude is small but small changes when it is large.

This consideration, however, does not take into account that electrons with different initial phases require different times (and distances) for deep deceleration. To account for this effect, we studied Eq. (22) again for electron beam parameters $\gamma_0=2$, $\alpha_0=1.5$, and the optimal phase velocity (refractive index) given by Eq. (15) and the optimal cyclotron resonance mismatch given by Eq. (24). Then the axial dependence of the efficiency,

$$\eta = \frac{1}{\gamma_0 - 1} \left\{ \gamma_0 - \frac{1}{2\pi} \int_0^{2\pi} \gamma(\xi) d\varphi_0 \right\}, \quad (25)$$

was computed for different distributions in initial phases φ_0 . First, we studied the case of a top-hat distribution of electrons in the range $\Delta\varphi_0$ around the "central" phase, $\bar{\varphi}_0$, i.e., the distribution function is constant for

$$\varphi_0 \in \left[\bar{\varphi}_0 - \frac{1}{2}\Delta\varphi_0; \bar{\varphi}_0 + \frac{1}{2}\Delta\varphi_0 \right]$$

and equals zero otherwise. Such a distribution corresponds to prebunching of electron beams for gyrodevices discussed elsewhere [41].

We have also studied the problem for more conventional methods of electron prebunching. As is known, the standard way of prebunching electrons is by weakly modulating the electron energies in the first (input) resonator, with successive ballistic phase bunching in the drift space. As a result, the electron distribution in phases at the entrance to the output interaction region has the form

$$\varphi(0) = \varphi_0 + q \sin \varphi_0 + \theta_{dr}, \quad (26)$$

where q is the bunching parameter proportional to the amplitude of the input signal and the drift length (see, e.g., [42]), and θ_{dr} is the electron transit angle through the drift region. If velocity spread is negligibly small, all electrons have the same θ_{dr} and this value can be eliminated from Eq. (26) by referring φ_0 to θ_{dr} . In a similar manner the ballistic phase bunching after two cavities and two drift regions can be described by the electron gyrophase distribution [43]

$$\varphi(0) = \varphi_0 + q_1 \sin \varphi_0 + q_2 \sin(\psi + \varphi_0 + r q_1 \sin \varphi_0), \quad (26a)$$

where q_1 and q_2 are bunching parameters proportional to field amplitudes in the first and second cavities, respectively, ψ is the difference between phases of these two fields, and the parameter $r = L_{dr,1} / (L_{dr,1} + L_{dr,2})$ determines the position of the penultimate cavity located at a distance $L_{dr,1}$ from the first cavity and at $L_{dr,2}$ from the output interaction region.

The axial dependence of the efficiency, Eq. (25), was studied for the same set of parameters, γ_0 , α_0 , β_{ph} , as earlier, and for the cases of one-cavity prebunching [with $q=1.8$ in Eq. (26) that is close to the optimal value of q]

and two-cavity prebunching [Eq. (26a) with $q_1=1.6$, $q_2=1.8$, $\psi=\pi/2$, and $r=0.95$; this set of parameters provides the maximum of the fundamental harmonic in electron current density at the entrance to the output section [43]].

Results are presented in Fig. 2. As shown in these figures, in the case of one-cavity prebunching the peak efficiency is approximately two times smaller than for an ideally prebunched beam (with $\Delta\varphi_0=0$). The utilization of a two-cavity prebunching scheme (with properly profiled magnetic field in drift regions) significantly improves the efficiency in comparison with the one-cavity prebunched scheme.

The important conclusion from Fig. 2 is that the optimal length for deceleration of initially 500 keV electrons by a large amplitude wave is on the order of wavelength. This means that for rapid deceleration of relativistic elec-

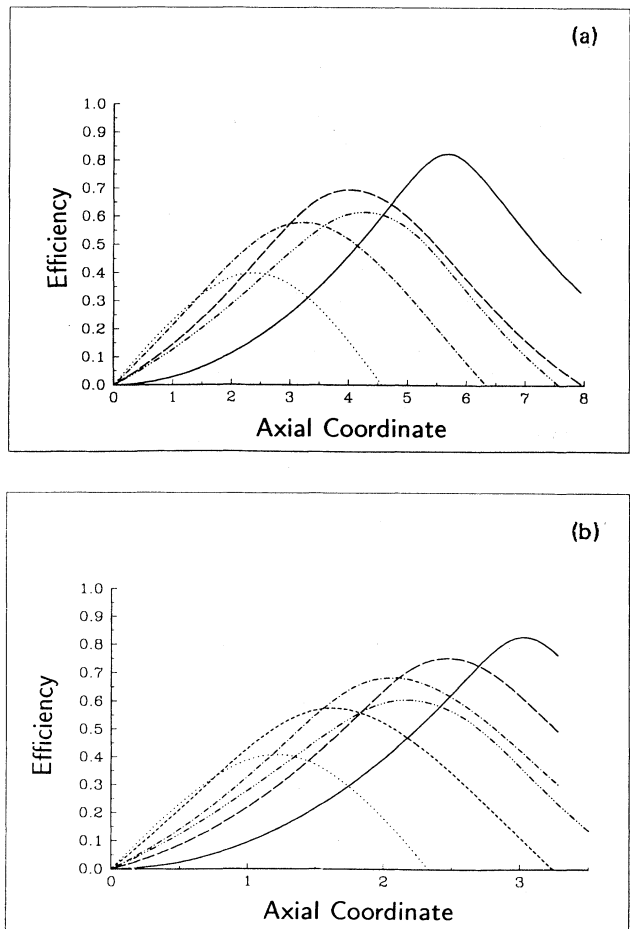


FIG. 2. Dependence of the efficiency on the normalized axial coordinate $\xi = \omega z / c$ for two values of the wave amplitude: (a) $a=0.1$, (b) $a=0.2$. Parameters' values are $\gamma_0=2$, $\alpha_0=1.5$, $n=n_{opt}=0.96$, $\delta=\delta_{opt}=0.1633$ (a) and 0.3 (b). Solid lines correspond to $\bar{\varphi}_0=0$, $\Delta\varphi_0=0$; dashed lines to $\bar{\varphi}_0=0$ and $\Delta\varphi_0=\pi/2$, dash-dotted lines to $\bar{\varphi}_0=0$ and $\Delta\varphi_0=\pi$. Dotted lines correspond to one-cavity prebunching with $q=1.8$; dot-dot-dashed lines correspond to two-cavity prebunching with $q_1=1.6$, $q_2=1.8$, $\psi=\pi/2$, and $r=0.95$.

trons an intense electromagnetic field is required. Indeed, the value of normalized amplitude, a , taken as equal to 0.2 for $\beta_{ph} = \beta_{ph, opt}$, $\gamma_0 = 2$, $\alpha_0 = 1.5$ corresponds to an electric field amplitude about 0.37 of that of the magnetostatic field (in gaussian units). Since such a high field can be difficult to realize because of microwave breakdown, there are at least two other options.

The first is to trap an electron bunch by a moderate amplitude wave and then decelerate this bunch gradually in a structure with properly tapered parameters. This kind of electron deceleration is realizable in cyclotron masers with tapered waveguides and magnetic field distributions.

The second option is to excite a strong electromagnetic field in a short resonator. Since the structure of such a field can be very different from the constant amplitude traveling wave considered above, we will study the interaction of gyrating electrons with resonator fields separately.

III. INTERACTION OF GYRATING ELECTRONS WITH STANDING WAVES IN RESONATORS

To simplify our analysis, let us suppose that the electrons make a large enough number of electron orbits in the resonator that we can use the equations for electron motion averaged over fast cyclotron gyration. (In the next section we will drop this assumption and consider several harmonics simultaneously.) At the same time, keeping in mind that the resonator length can be rather short, we will take into account effects caused by the axial inhomogeneity of the resonator field. Since cyclotron masers operate at TE rather than at TM modes (see, e.g., [14]) we will consider below only the interaction of electrons with the TE modes. As shown elsewhere [17], this consideration can be adopted to the case of TM modes.

The electric and magnetic field of any resonator mode oscillating in a stationary regime can be presented as

$$\mathbf{E} = \text{Re}\{ A \mathbf{E}_s e^{i\omega t} \}, \quad \mathbf{B} = \text{Re}\{ A \mathbf{B}_s e^{i\omega t} \},$$

where ω is the frequency of electromagnetic oscillations, A is the field amplitude, and \mathbf{E}_s and \mathbf{B}_s describe spatial structures of electric and magnetic fields, respectively. These functions can be expressed via the Hertz potential Φ_A , which is the solution of the Helmholtz equation $\Delta \Phi_A + (\omega/c)^2 \Phi_A = 0$ supplemented with the appropriate boundary conditions. In the case of TE modes, \mathbf{E}_s and \mathbf{B}_s are written

$$\mathbf{E}_s = \frac{c}{\omega} [\nabla_{\perp} \Phi_A \times \hat{\mathbf{z}}_0],$$

$$\mathbf{B}_s = i \{ \Phi_A \hat{\mathbf{z}}_0 + \frac{c^2}{\omega^2} \text{grad div}(\Phi_A \hat{\mathbf{z}}_0) \}.$$

Below we will assume that axial variations in the resonator profile are weak enough that the potential function, Φ_A , has the functional form $\Phi_A = \Psi(x, y, z) f(z)$. Here $\Psi(x, y, z)$ is the membrane function describing the transverse structure of oscillations. It depends weakly on z and satisfies the membrane equation $\Delta_{\perp} \Psi + k_{\perp}^2(z) \Psi = 0$ with the boundary condition that the normal derivative

of Ψ at the wall vanishes. The transverse wave number k_{\perp} depends on z only when the wall radius does. The function f describes the axial structure of the resonator field. If the effect of an electron beam on the axial structure of the resonator is negligibly small (the so-called "cold-cavity" approximation, which is valid when the reflections of the field from the input and output cross sections of the resonator are large enough), this function satisfies the equation

$$\frac{d^2 f}{dz^2} - \left[\frac{\omega^2}{c^2} - k_{\perp}^2(z) \right] f = 0$$

known as the inhomogeneous string equation [44]. This equation should be supplemented with the boundary conditions that the evanescent field at the input cutoff cross section vanish as $z \rightarrow \infty$, and that the backward wave vanish at the output cross section where the open resonator is coupled to the output waveguide (see, e.g., [44]).

To study the resonant interaction between gyrating electrons and the high-frequency electromagnetic field, it is expedient to use the Fourier expansion of the membrane function Ψ in terms of harmonics of angular coordinate θ (see, e.g., [8,14]) in the vicinity of an electron guiding center with coordinates X_g, Y_g

$$\Psi = \sum_s \Psi_s(X_g, Y_g, r_L) e^{-is\theta}, \quad (27)$$

where X_g, Y_g, r_L , and θ are related to the transverse coordinates x and y by

$$x = X_g + r_L \cos\theta, \quad y = Y_g + r_L \sin\theta.$$

The quantity r_L is to be interpreted as the electron Larmor radius, $r_L = v_{\perp}/\Omega_c$. Using the integral representation of Bessel functions (Graff's theorem) the coefficients Ψ_s in Eq. (27) can be written [45]

$$\Psi_s = J_s(k_{\perp} r_L) L_s(X_g, Y_g), \quad (28)$$

where the Bessel function $J_s(k_{\perp} r_L)$ gives the amplitude of the s th-order multipole at distance r_L from the center of its angular rotation. Usually the argument $k_{\perp} r_L$ is small enough ($k_{\perp} r_L < s$) that the Bessel function can be approximated by the s th-order polynomial. The operator

$$L_s = \left[\frac{s}{|s|} \right]^s \left[\frac{1}{k_{\perp}} \left[\frac{\partial}{\partial X_g} + i \frac{s}{|s|} \frac{\partial}{\partial Y_g} \right] \right]^{|s|} \Psi(X_g, Y_g) \quad (29)$$

describes the transverse structure of the corresponding harmonic of the membrane function at the point with coordinates X_g, Y_g . For cylindrical resonators a membrane function of the $TE_{m,p}$ mode is $J_m(k_{\perp} r) e^{-im\psi}$. Correspondingly, the operator L_s is equal to $L_s = J_{m \mp s}(k_{\perp} r_g) e^{i(m \mp s)\psi_g}$, where r_g and ψ_g are related to X_g and Y_g as $X_g = r_g \cos\psi_g$, $Y_g = r_g \sin\psi_g$, and the signs $-$ and $+$ correspond, respectively, to the rotation of the gyrating electrons in the same and opposite directions as the operating mode.

For the representation of the resonator electromagnetic field given above one can average the equations for electron motion (8) and (9) over fast gyration and arrive

at the reduced set of average equations given in [46]

$$\frac{d\gamma}{d\xi} = \frac{p_\perp^s}{p_z} \operatorname{Re}\{F f e^{i\varphi}\}, \quad (30a)$$

$$\frac{dp_z}{d\xi} = \frac{p_\perp^s}{p_z} \operatorname{Re}\left\{iF \frac{df}{d\xi} e^{i\varphi}\right\}, \quad (30b)$$

$$\frac{d\varphi}{d\xi} = \frac{\gamma - s\gamma_0\Omega_{c0}/\omega}{p_z} = s\gamma \frac{p_\perp^{s-2}}{p_z} \operatorname{Re}\left\{F e^{i\varphi} \left[i f + \frac{p_z}{\gamma} \frac{df}{d\xi}\right]\right\}. \quad (30c)$$

Here s is the resonant cyclotron harmonic number, and the slowly varying quantity $\varphi = \omega t - s\theta$ is the particle phase with respect to the phase of the resonator field. As earlier, components of electron momentum are normalized to $m_0 c$ and p_\perp can be determined as $p_\perp = (\gamma^2 - 1 - p_z^2)^{1/2}$. The normalized amplitude of the resonator field, F , is equal to

$$F = \frac{eA}{m_0 c \omega} \frac{1}{(s-1)! 2^{s+1}} \frac{(k_{10} c / \omega)^{s-2}}{(\gamma_0 \mu)^{s-1}} L_s. \quad (31)$$

Equation (30b) describes the dependence of the electron axial momentum on the axial inhomogeneity of the field structure. Recall that the axial field structure in resonators can usually be represented as the superposition of many plane, transversely inhomogeneous waves propagating with different axial wave numbers (see, e.g., [45]). This makes the consideration of the interaction between electrons and resonator fields more complicated than that in waveguides. Nevertheless, there is at least one partial case when this interaction is essentially the same: consider a sinusoidal axial structure with a large number of field variations along the resonator length and assume that the cyclotron resonator condition (1) is valid for a forward wave component. Then the backward wave component can be neglected and Eqs. (30) for the case of fundamental cyclotron resonance are reduced to Eqs. (11).

Equations (30a)–(30c) are valid for an arbitrary axial structure of the resonator field and arbitrary cyclotron harmonic. We have studied them for the simplest case of a sinusoidal axial structure, $f(\xi) = \sin[\pi(\xi/\xi_{\text{out}})]$, and operation at the fundamental cyclotron resonance ($s = 1$). We considered a monoenergetic beam both with and without spread in orbital velocities. This set of equations was again supplemented with the expression for the electron efficiency (25) and with the general relation between electron energy and momentum (13).

To study the effect of deceleration of electron bunches in the resonator we also need to specify the phase distribution of electrons at the entrance. We have considered two schemes: a free running, single resonator oscillator (gyromonotron) in which the electrons are distributed homogeneously in phase, and a two-cavity gyrokylystron with the boundary conditions given by Eq. (26).

The set of equations (30a)–(30c), with corresponding boundary conditions, was studied for the initial normalized electron energy $\gamma_0 = 2$, pitch factor $\alpha_0 = 1.5$, and

electron bunching parameter $q = 0$ and 1.8. Results are presented in Fig. 3, where lines of equal efficiency optimized with respect to the magnetic field parameter, δ_0 , are shown in the plane of normalized amplitude, F , and

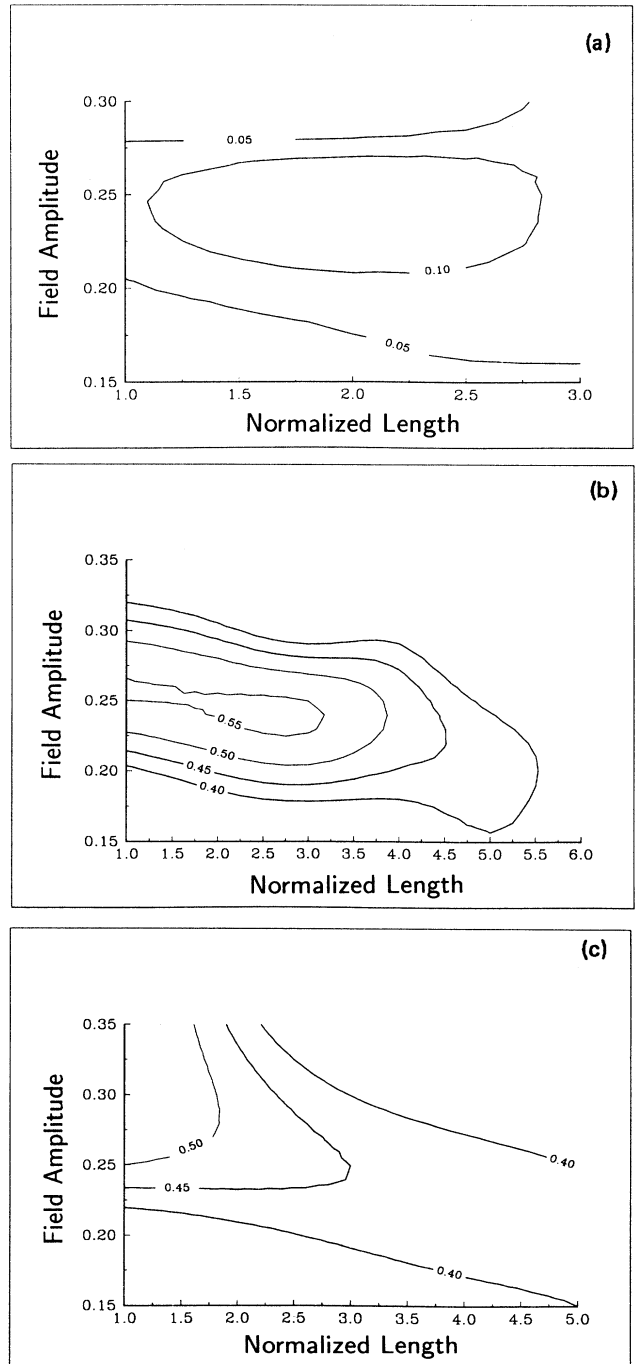


FIG. 3. Interaction efficiency of cyclotron maser schemes with a $\gamma_0 = 2$, $\alpha_0 = 1.5$ electron beam: (a) monotron with no velocity spread, (b) klystron with no velocity spread and one-cavity prebunching, $q = 1.8$, (c) klystron with one-cavity prebunching, $q = 1.8$ and 6% orbital velocity spread (it is assumed that in the last scheme the external magnetic field is profiled for discrimination of velocity spread effects in a drift region).

length, ξ_{out} . Figures 3(a) and 3(b) correspond to an ideal electron beam with no velocity spread. In Fig. 3(a) the case of gyromonotron is shown, e.g., $q=0$; Fig. 3(b) corresponds to a gyrokylystron with $q=1.8$. Figure 3(c) shows the efficiency of a gyrokylystron with the same bunching parameter ($q=1.8$) and a monenergetic beam with a triangular distribution in orbital velocities, corresponding to an rms spread of 6%. The results shown in Fig. 3(c) are obtained under the assumption that, due to the profiling of the external magnetic field, the transit angle through the drift region, θ_{dr} , given in Eq. (25) is equal to zero, and therefore the spread in electron axial velocities does not cause a spread in input phases $\theta(0)$.

From Fig. 3 it follows, first, that electron prebunching drastically increases the electron efficiency. Second, when the effect of electron axial velocity spread on transit angles through the drift space is compensated for by proper profiling of the guiding magnetic field, the efficiency degradation caused by velocity spread is rather weak. Third, the optimal interaction length in all cases shown in Fig. 3 is short in accordance with Eq. (6). Such a short length leads to a strong axial inhomogeneity of the electric field structure. According to Eq. (30b) this inhomogeneity may cause significant changes in electron axial momentum which increase the efficiency. For illustration the axial dependence of electron axial momenta is shown in Fig. 4 for gyrokylystron with an ideal electron beam (parameters are $\xi_{\text{out}}=3$, $F=0.24$, $\Omega_{c0}/\omega=0.8$, $q=1$, $\gamma_0=2$, $\alpha_0=1$). For this set of parameters the efficiency is about 44% and, as is seen from Fig. 4, electrons undergo significant changes in p_z . However, at such a short distance the electrons make less than one turn in the external magnetic field. Therefore, to describe such an interaction between electrons and the em field adequately we have to use nonaveraged equations of electron motion and take into account the interaction of the electrons with the electromagnetic field at several cyclotron harmonics simultaneously. This has been done in realistic designs (where space charge effects were also tak-

en into account) [26–29]. Below, we will discuss some of the principal issues in this complicated matter.

IV. SIMULTANEOUS INTERACTION OF ELECTRONS WITH RESONATOR FIELDS AT SEVERAL CYCLOTRON HARMONICS

A general description of the simultaneous interaction between electrons and electromagnetic fields at several cyclotron harmonics is not simple. First, we cannot average the equations for electron motion over a cyclotron period, so these equations contain a large number of parameters. Second, when the number of electron orbits in the interaction space is small the transverse drift of electron guiding centers is of the same order as changes in electron energy and momentum. Therefore this drift must also be taken into account. However, we will not go into all the details here but will illustrate this issue with a few simple examples.

First of all, let us attempt to account for the simultaneous interaction at several harmonics by a method of successive approximation. By this we mean that we will keep in the equations for electron motion, besides the field of an originally resonant cyclotron harmonic, s , also the terms responsible for the interaction with neighboring harmonics, $s-1$ and $s+1$. Then, for the simplest case of operation near cutoff at $s=2$ one can get instead of Eqs. (30) the following set of equations (for other harmonics, these equations have a similar form):

$$\frac{d\gamma}{d\xi} = \frac{p_{\perp}^2}{p_{z0}} \operatorname{Re}\{Ffe^{i\omega t}[b_1e^{-i\theta}p_{\perp}^{-1} + e^{-i2\theta} + b_3p_{\perp}e^{-i3\theta}]\}, \quad (32a)$$

$$\frac{d\theta}{d\xi} = \frac{\Omega_{c0}}{\omega} \frac{\gamma_0}{p_{z0}} - \frac{\gamma}{p_{z0}} \operatorname{Re}\{iFfe^{i\omega t}[b_1p_{\perp}^{-1}e^{-i\theta} + e^{-i2\theta} + b_3p_{\perp}e^{-i3\theta}]\}. \quad (32b)$$

Here, parameters b_1 and b_3 are responsible for the first and third cyclotron harmonic interaction, respectively:

$$b_1 = \frac{2\Omega_{c0}}{\omega} \left| \frac{L_1}{L_2} \right|, \\ b_2 = \frac{\omega}{4\Omega_{c0}} \left| \frac{L_3}{L_2} \right|,$$

where L is defined in Eq. (29). We do not present here equations for p_{\perp} and p_z , since for operation near cutoff $p_z \simeq \text{const} = p_{z0}$ and, therefore, the changes in p_{\perp} and γ are related as $p_{\perp}(dp_{\perp}/d\xi) = \gamma(d\gamma/d\xi)$. Since the cyclotron frequency of decelerated electrons is larger than its unperturbed value, these electrons become shifted from initial closeness to the second harmonic towards fundamental resonance. Correspondingly, accelerating electrons decrease their cyclotron frequency, which makes the third harmonic interaction for these particles more pronounced (when $\omega t - 3\theta$ varies slowly).

The resulting effect from interaction with other harmonics obviously depends first on electron prebunching and second on the initial mismatch of cyclotron reso-

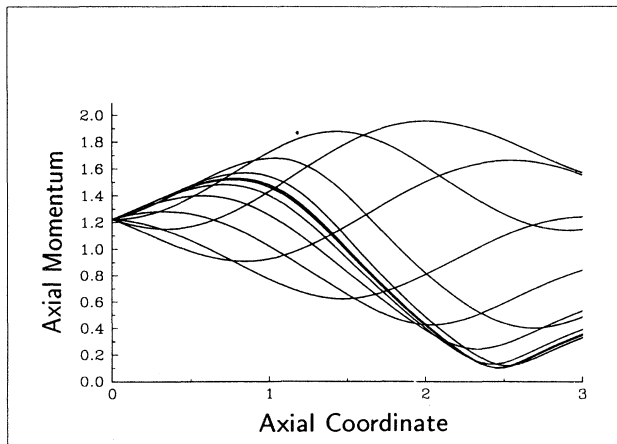


FIG. 4. Axial dependences of electron axial momenta in the output cavity of a gyrokylystron with no velocity spread and $\gamma_0=2$, $\alpha_0=1$, $q=1$, $\xi_{\text{out}}=3$, $F=0.24$, $\mu=0.8$ (for this set of parameters the efficiency is about 44%).

nance. For a single harmonic interaction this mismatch is usually rather large. It means that one places pre-bunched electrons near the top of the “cat’s eye” shown in Fig. 5 and then gains energy from sending them to its bottom. In such a case for electrons starting in a “wrong” phase (outside the separatrix, see Fig. 5), the third harmonic may accelerate them and thus spoil the interaction efficiency. Let us point out that in the reference frame related to the second harmonic interaction the phase space corresponding to the fundamental harmonic moves to the right while that corresponding to the third harmonic moves to the left. So, an electron initially outside can be trapped by the slipping harmonic “cat’s eye”

only when the field amplitude is large enough to make significant changes in its energy and phase.

Let us illustrate this discussion with consideration of “klystron” model of interaction. In such a model, originally suggested for a qualitative analysis of gyrotron nonlinearities by Yulpatov, the interaction space consists of two short gaps with the same microwave field in each, separated by a drift region. For such a model, Eqs. (32) can be integrated analytically. When the field amplitude is small enough and all nonlinearity is caused by ballistic bunching in a drift region only, the corresponding expression for the electron efficiency optimized with respect to the drift transit angle has the following form:

$$\eta = \frac{F}{\gamma_0 - 1} \operatorname{Re} \{ \langle \langle (1 + \bar{b}_1 e^{i\psi_0} + \bar{b}_3 e^{-i\psi_0}) e^{i\{\bar{\varphi}_0 + q \operatorname{Re}[e^{i\bar{\varphi}_0} (1 + \bar{b}_1 e^{i\psi_0} + \bar{b}_3 e^{-i\psi_0})]\}} \rangle \rangle \}. \quad (33)$$

Here the bunching parameter q has the same meaning as in Eq. (26). Double angular brackets mean averaging over normalized entrance time $\bar{\varphi}_0$ and initial gyroangle ψ_0 . The parameters $\bar{b}_{1,3}$ are defined as $\zeta b_{1,3}$ where $\zeta = [\sin(\Theta_1/2)/(\Theta_1/2)]$ is the standard klystron parameter describing transit effects in a short gap [$\Theta_1 = (1 - s\Omega_{c0}/\omega)L_1/\beta_{z0}$ is the transit angle in one gap of length L_1]. After integration over $\bar{\varphi}_0$ Eq. (33) becomes equal to

$$\eta = \frac{F}{\gamma_0 - 1} \langle (1 + b_1 e^{i\psi_0} + b_3 e^{-i\psi_0}) J_1[q(1 + b_1 e^{i\psi_0} + b_3 e^{-i\psi_0})] \rangle. \quad (34)$$

At small b_1, b_3 the expression in angular brackets denoted as $\bar{\mathcal{J}}$ being expanded in b_1, b_3 and averaged over ψ_0 can be reduced to

$$\begin{aligned} \bar{\mathcal{J}} &= J_1(q) + b_1 b_3 [q J'_1(q) - (q^2 - 1) J_1(q)] \\ &= J_1(q) + b_1 b_3 q [J_0(q) - q J_1(q)]. \end{aligned} \quad (35)$$

So, when the bunching parameter q is optimal for single-harmonic interaction ($q_{\text{opt}} \simeq 1.84$, see [42]) the presence of other harmonics only deteriorates the efficiency. How-

ever, at small q [when $q J_1(q) < J_0(q)$], these harmonics may improve the efficiency. More accurate numerical analysis of gyrodevices with simultaneous interaction of electrons with microwave fields at several harmonics was described in [27].

Let us also mention another specific case related to simultaneous interaction of electrons with a resonator field at two cyclotron harmonics (our attention was called to this case by S. Tantawi). Suppose for simplicity that the resonator field has a sinusoidal axial structure $f(x) = \sin(l\pi z/L)$ and, therefore, can be represented as the superposition of two opposite waves with the axial wave number $k_z = \pm l\pi/L$. One can easily find that both of these waves may be in cyclotron resonance with electrons. For instance, the forward wave may be in resonance at the s th harmonic while the opposite one at the $(s+1)$ th harmonic. This operation corresponds to the Doppler frequency upshift, $\omega/\Omega_c = (2s+1)/2$, or, in other words, to the axial index

$$l = \frac{2}{2s+1} \frac{L/\lambda}{\beta_{z0}}. \quad (36)$$

As one can see, for relativistic electron axial velocities and a short resonator length, this index may be equal to 1 or 2. Thus such a double resonance can easily be realized in standard gyrotron cavities with the normalized length $L/\lambda = l(2s+1)\beta_{z0}/2$. Apparently, when the axial electron velocity is small, this resonance may occur in long cavities only if the operating mode has a large number of axial variations.

Now let us describe in a few words another limiting case: the “relay” interaction of initially ultrarelativistic electrons with a succession of cyclotron harmonics in the

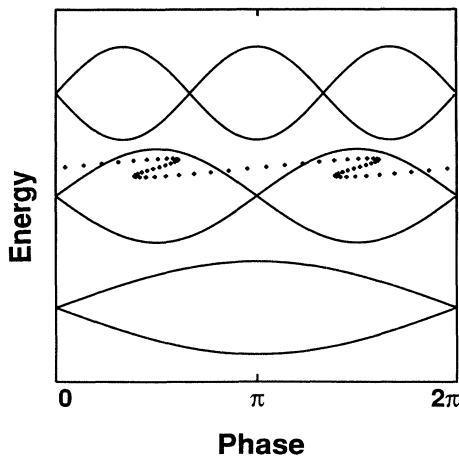


FIG. 5. Illustration of the possible interaction at the first and third cyclotron harmonics in relativistic cyclotron masers designed for operation at the second harmonic (fundamental resonance may take place here only when the operating voltage is high enough.)

process of synchrotron radiation. The nonlinear (or, more exactly, quasilinear) theory of such a synchrotron maser was developed in Ref. [47], in which the authors consider a beam with a large spread in electron energy. Due to this spread in energy, at a given instant of time different electron fractions have different cyclotron frequencies, and hence interact with the electromagnetic wave at different cyclotron harmonics. The synchrotron maser studied in [47] was described by a pair of equations for the field intensity and the electron distribution function. It was found that depending on the derivative of the diffusion coefficient with respect to electron energy, the electron beam may lose or gain energy in the process of interaction with the wave. The gain is possible only in systems far from exact autoresonance when this derivative is negative. These results demonstrate a common nature of the studied synchrotron instability with the cyclotron maser instability [1,5,32] which occurs due to the negative derivative of the electron-cyclotron frequency with respect to its energy. The efficiency of such a synchrotron maser with large initial electron energy spread and successive relay interaction is about 6% or less [47].

To further illustrate the effect of interaction with more than one harmonic, we performed simulations using Eq. (32) above. For definiteness, we took the dominant harmonic to be $s=2$ and included competition from the third harmonic only; i.e., set $b_1=0$ in Eq. (32). This is valid in realistic scenarios in which the particles are placed initially near the top of the second harmonic separatrix to ensure that they lose energy, and thus far from the first harmonic resonance. Our strategy was to first set the third harmonic coupling, b_3 , to zero and compute the efficiency versus cavity length. At each length, the efficiency was optimized with respect to the amplitude and phase of F , the bunching parameter, q , and the frequency mismatch, $1-2\Omega_{c0}/\omega$. (The factor of 2 indicates that the second harmonic is dominant.) It was taken as an rms axial velocity spread of 7%. We then repeated the optimization procedure with finite third harmonic interaction; i.e., b_3 ranging from 0.1 to 0.6 in steps of 0.1. Figure 6(a) indicates that as b_3 increases the peak efficiency decreases, with the peak efficiency moving to larger lengths. Figures 6(b) and 6(c) show also that as the length increases both the amplitude and the frequency mismatch decrease. This is consistent with our picture of overlapping of resonances: as the third harmonic interaction becomes more important, the amplitude decreases to reduce the degree of resonance overlap, and the frequency mismatch decreases so that the particles are initially lower in the separatrix.

V. CYCLOTRON MASERS WITH VARIABLE MAGNETIC FIELDS

As mentioned above, the cyclotron resonance between the wave and gyrating relativistic electrons can be maintained in the process of interaction if the electromagnetic wave propagates along \mathbf{B}_0 with phase velocity close to the speed of light. As shown in Refs. [19,20,30], the interaction of ideal (no velocity spread) electron beams with such waves in CARMs can be rather efficient. However,

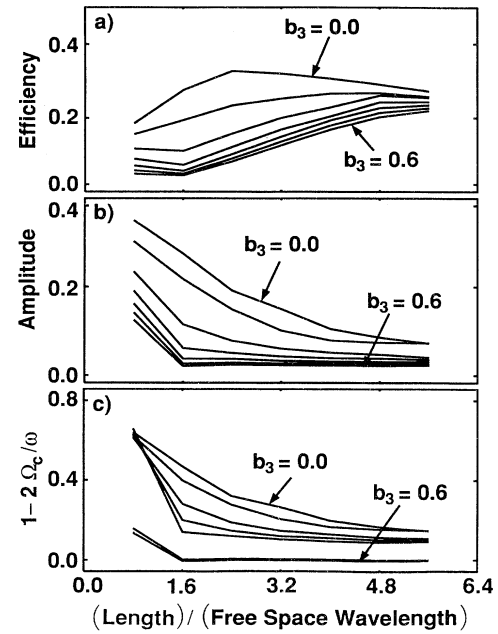


FIG. 6. Effect of the third harmonic interaction on the operation of a second harmonic cyclotron maser with a 425 kV, $\alpha_0=1$ electron beam; the resonator length is related to the wavelength.

as follows from Eq. (7), in this kind of interaction the axial velocity spread inherent in typical electron beams used in cyclotron masers leads to significant inhomogeneous Doppler broadening of the cyclotron resonance band and, therefore, degrades efficiency. This sensitivity was confirmed in a number of theoretical studies [48–50] and it may be considered the main reason for low efficiencies observed in CARM experiments [21,22]. (Note that the highest efficiency, 10%, was realized in a CARM with a nontraditional electron optics providing better beam quality [21].) Also important is an increase in the group velocity of the wave, $v_{gr}=c^2/v_{ph}$, that reduces coupling of the wave to electrons. To provide optimal electron bunching in this case one has either to increase the beam current, which may enhance the role of space charge effects in deteriorating efficiency, or to increase the interaction length, which makes the interaction more sensitive to electron velocity spread.

We may conclude, then, that it is reasonable to operate at waves with smaller axial wave numbers than required for CARM operation (in order to reduce the sensitivity of efficiency to electron axial velocity spread) but with a tapered magnetic field to maintain cyclotron resonance. As follows from Eq. (7), to maintain resonance with decelerating particles the magnetic field must be down-tapered. Such tapering works as a kind of phase selection since electrons entering the interaction space in a decelerating phase can be trapped by the wave and interact with it for a long time, while those entering in an accelerating phase will soon be out of resonance due to rapid changes in cyclotron frequency. Of course, the num-

ber of trapped particles can be increased by electron pre-bunching which leads us to the relativistic gyrotwistron [46,51]. This device combines bunching cavities separated by drift regions used in gyrokylystrons with the output waveguide of the gyro-traveling-wave-tube. The merits of this device will be discussed later. Now we will discuss the basic features of interaction between electromagnetic waves and relativistic electrons gyrating in a tapered magnetic field.

For the simple model considered above with a constant magnetic field (Sec. II) the equations for electron motion in the case of a tapered magnetic field can be written as (cf. Ref. [24])

$$\frac{dp_{\perp}}{d\xi} = -\frac{\gamma - np_z}{p_z} \operatorname{Im}(Ae^{-i\varphi}) + \frac{gp_{\perp}\gamma}{p_z}, \quad (37a)$$

$$\frac{d\varphi}{d\xi} = \frac{1}{p_z} \left[\frac{\omega - k_z v_z - \Omega_c}{\omega} - \frac{\gamma - np_z}{p_{\perp}} \operatorname{Re}(Ae^{i\varphi}) \right], \quad (37b)$$

$$\frac{dp_z}{d\xi} = -n \frac{p_{\perp}}{p_z} \operatorname{Im}(Ae^{i\varphi}) - g\gamma \frac{p_{\perp}^2}{p_z^2}, \quad (37c)$$

$$\frac{d\gamma}{d\xi} = -\frac{p_{\perp}}{p_z} \operatorname{Im}(Ae^{i\varphi}). \quad (37d)$$

In comparison with Eqs. (11a)–(11d) given above for a constant magnetic field model, Eqs. (37a)–(37d) contain some new terms proportional to the parameter of tapering

$$g = \frac{1}{2B_0} \frac{dB_0}{d\xi}.$$

In principle, one should supplement these equations with the equations describing transverse drift of electron guiding centers in a waveguide field. Such equations were derived in [24]. However, for simplicity, we will ignore this effect here.

Now, as follows from Eqs. (37c) and (37d), instead of the integral of motion given by Eq. (12) the following relation between electron energy and axial momentum is valid:

$$n \frac{d\gamma}{d\xi} = \frac{dp_z}{d\xi} + g \frac{p_{\perp}^2}{p_z \beta_z}. \quad (38)$$

Also the electron energy and transverse momentum are related by [24]

$$\frac{dp_{\perp}^2}{d\xi} = (1 - n\beta_z) \frac{d\gamma^2}{d\xi} + \frac{2gp_{\perp}^2}{\beta_z}. \quad (39)$$

In Eqs. (38) and (39), the last terms describe magnetic compression (decompression) of electrons in the up-tapered (down-tapered) external magnetic field. Note that in the case of the down-tapered magnetic field the decompression of electrons means reduction of their orbital velocities and, correspondingly, enhancement of their axial velocities. On the one hand, it may help to avoid the appearance of reflected particles in regimes of deep deceleration, but on the other hand, it reduces the energy of the electron gyration available for transformation into microwave energy. To compensate for this

reduction one can slow down the phase velocity of the wave, which is the opposite of our initial tendency to operate at waves with large phase velocities (small k_z). Let us discuss this issue in more detail.

Let us distinguish an electron, which we will suppose to move with constant phase with respect to the wave, and let us call it the “synchronous” electron. As follows from Eq. (37b), the synchronism between this electron and a wave with small amplitude [when the last term in Eq. (37b) can be ignored] means

$$\Omega_c = \omega - k_z v_z.$$

Introducing μ' as the ratio of nonrelativistic electron-cyclotron frequency to the wave frequency, one can rewrite this equation as

$$\mu' = \gamma_s - np_{z,s} \quad (40)$$

(here, s means “synchronous”). Equation (40) shows us how to profile the external magnetic field in order to maintain synchronism with the synchronous electron. Note that Eq. (40) is also valid for the case when the wave phase velocity (refractive index n) is variable. Using Eq. (40) to define the value of g according to changes in the energy and axial momentum of the synchronous electron, one can readily get for the synchronous electron the following integral of motion [24]:

$$2\gamma_s - \frac{p_{\perp,s}^2}{\gamma_s - np_{z,s}} = \text{const} = 2\gamma_0 - \frac{\gamma_0 \beta_{10}^2}{1 - n_0 \beta_{z0}}. \quad (41)$$

This equation can also be interpreted as the dependence of the orbital momentum of the synchronous electron on its energy and axial velocity:

$$p_{\perp,s}^2 = \frac{\gamma_s}{\gamma_0} \frac{1 - n\beta_{z,s}}{1 - n_0\beta_{z0}} p_{10}^2 - 2(1 - n\beta_{z,s})\gamma_s(\gamma_0 - \gamma_s), \quad (42)$$

which is similar to Eq. (14) derived for a constant magnetic field and wave phase velocity. Equation (41) leads to an expression for the single-particle efficiency of the synchronous electron that is the same as the one given in Eq. (18) for a constant magnetic field,

$$\eta_{s,SP} = \frac{\gamma_0 - \gamma_f}{\gamma_0 - 1} = \frac{\beta_{10}^2}{2(1 - \gamma_0^{-1})(1 - n_0\beta_{z0})}. \quad (43)$$

Here, γ_f is the final energy of an electron losing its orbital momentum. Note that our system of averaged equations has a Hamiltonian from which the integral of motion follows [52]:

$$\gamma - \frac{\omega}{s\Omega} P_{\perp}^2 = \text{const},$$

where P_{\perp} is the canonical momentum normalized to m_0c . Therefore, supposing that the maximum extraction of electron energy corresponds to zero orbital momentum at the final stage, one can find for the single-particle efficiency the equation

$$\eta_{SP} = \frac{\beta_{10}^2}{2(1 - \gamma_0^{-1})} \frac{\omega}{\Omega_c},$$

which near cyclotron resonance coincides with Eq. (43).

The difference between Eqs. (42) and (14), which corresponds to the necessity of slowing down the optimal phase velocity of the waves discussed above, leads to the conclusion that in the case of the tapered external magnetic field the optimal wave is always the slow one (at least, at the entrance to the interaction region). Indeed, as follows from Eq. (43), the single-particle efficiency of the synchronous electron is equal to unity when the initial refractive index is equal to [24]

$$n_0^{\text{opt}} = 1 + \frac{(1 - \gamma_0^{-1} - \beta_{z0})^2}{2\beta_{z0}(1 - \gamma_0^{-1})}. \quad (44)$$

Equation (44) shows that, in general, it is optimal to operate at slow waves ($n_0^{\text{opt}} > 1$) under the condition of the normal Doppler effect ($n_0^{\text{opt}} \beta_{z0} < 1$). (There is also one partial case of $\beta_{z0} = 1 - \gamma_0^{-1}$ when $n_0^{\text{opt}} = 1$, and the optimal interaction is with a wave traveling at the speed of light; see [10,11].) In the case of total particle deceleration ($\gamma_f = 1$), the axial momentum is a linear function of electron energy

$$p_{z,s}(n_0^{\text{opt}}) = (\gamma_s - 1)[n_0^{\text{opt}} + \sqrt{(n_0^{\text{opt}})^2 - 1}] \quad (45)$$

similar to cyclotron masers with constant magnetic field and phase velocity, for which the integral given by Eq. (12) is valid.

Of course, for practical purposes we should take into account such factors as the previously discussed electron axial velocity spread and the desire to avoid the appearance of reflected particles. Then, we readily come to the conclusion that the phase velocity must be larger than the optimal one. [A corresponding dependence of the shift in phase velocities on the axial velocity spread can be estimated from Eqs. (1) and (7).] Therefore practical configurations of cyclotron masers can be designed for efficient operation not only at slow waves (see, e.g., [56]) but also at widely used fast waves.

Note that even when electron velocity spread produced by electron guns is negligibly small, there will be a certain spread in energies of electrons starting interaction with the wave at different gyrophases. When this spread in energies is small enough the electron phases obey the nonlinear pendulumlike equation [23,24]

$$\frac{d}{d\xi} \left[M \frac{d\varphi}{d\xi} \right] = K(\sin\varphi - \sin\varphi_s). \quad (46)$$

Here φ_s is the phase of the synchronous electron; the coefficient M , called the effective mass of the oscillator, depends on energy and axial momentum of electrons as well as on the refractive index n ; the coefficient K , known as the coefficient of elasticity, is proportional to the amplitude of the electromagnetic Lorentz force acting on electrons and also depends on momentum components of the synchronous electron [23,24]. Equation (46) is known in the theory of cyclic accelerators as the equation for synchrotron oscillations. Bounce oscillations of electrons described by Eq. (46) can be interpreted as oscillations of charged particles in the potential well whose shape depends on the phase of synchronous electron φ_s . The optimal choice of φ_s in turn depends on parameters of elec-

tron prebunching [24] as well as on restrictions on the interaction length caused by self-excitation of parasitic waves in long waveguides.

Note that Eqs. (41)–(45) discussed above do not describe all the details of electron-wave interaction. To define the tapering of the magnetic field given by Eq. (40) we must know the changes in the electron energy and axial momentum which, in turn, depend on the magnetic field tapering (so, this is a self-consistent problem), on the wave amplitude, and other parameters of the interaction region.

To find the axial dependence of the wave amplitude we should consider the equation for wave excitation with the source term averaged over particle distribution in all initial parameters (initial gyrophases and others). Such an equation for relativistic cyclotron masers with traveling waves has been derived elsewhere [53,54]. In the variables used in Eq. (37) this equation has the form

$$\frac{dA}{d\xi} = i \frac{\omega_p^2}{\omega^2} \frac{p_{z0}}{n} \frac{1}{2\pi} \int_0^{2\pi} \frac{p_\perp}{p_z} e^{-i\varphi} d\varphi_0, \quad (47)$$

where ω_p is the electron plasma frequency. In principle, not only the absolute value of A but also its phase vary along ξ . However, since phases appear only in the combination denoted φ , the change in the wave phase can be accounted for in Eq. (11b) by adding the corresponding term, which can be found from the imaginary part of Eq. (47) (see [24,55]). Note that the departure from operation near cutoff, as follows from Eq. (47), reduces the coupling of electrons to the wave. Thus, in real experiments the value of n (or axial wave number) must be chosen taking into account the available beam current and the restriction on the interaction length discussed above.

The interaction of a prebunched electron beam with a traveling wave in a tapered external magnetic field has been realized in gyrotron experiments performed at the University of Maryland [51]. In these experiments, a strongly tapered magnetic field was used to maximize energy extraction. The experiment employed a 430 kV, 160–220 A beam with a pitch ratio near 1. Shown in Fig. 7 is the design magnetic field and the optimal experimental one, along with the placement of the input cavity and waveguide. In the experiment there were four independently adjustable sets of magnetic field coils: one in the gun region (which controlled the velocity ratio) and three in the circuit region. The efficiency was optimized

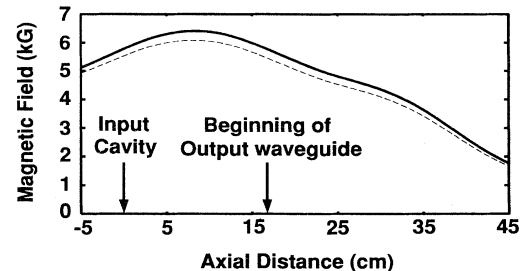


FIG. 7. Optimal magnetic field profiles found in the design (solid line) and experimentally (dashed line).

as follows: the three sets of circuit coils were fixed and the gun coil magnetic field was slowly decreased (thus increasing the velocity ratio). Initially as the velocity ratio increased so did the efficiency, but eventually parasitic oscillations were induced which drastically reduced output power. At this point new values were chosen for the circuit coils and the above procedure was repeated. The peak efficiency, which occurred at the magnetic field profile shown in Fig. 7 and a current of 220 A, was 22%, corresponding to an output power of about 22 MW. The agreement between the theoretical and experimental optimal axial distributions of the magnetic field looks quite satisfactory. Note that in this experiment an uptapered output waveguide section was used in which the ratio $k_z c / \omega = n$ was varied from about 0.3 at the entrance to about 0.5 at the exit.

VI. SUMMARY

Using simple models we considered some basic phenomena in the interaction of relativistic gyrating electrons with electromagnetic waves. Using the formalism developed earlier for electron autoresonance acceleration we studied deceleration of gyrating relativistic electrons by electromagnetic waves. The optimum cyclotron resonance mismatch was found. The spread in initial gyro-phases causing significant degradation in the efficiency of electron deceleration was estimated.

It was shown that the interaction of relativistic electrons with a resonator field is most efficient when the resonator length is short and the field amplitude is high.

In such a situation, the resonator electric field may have rather strong axial inhomogeneity. This inhomogeneity causes the appearance of the transverse magnetic field of the resonator, which leads to axial deceleration of electrons. This effect may enhance the efficiency. However, for too short interaction length, simultaneous interaction of electrons with the field at several cyclotron harmonics can be important. As was shown for second harmonic gyrokylystrons, this overlapping of resonance can lead to efficiency degradation. Note also that the field amplitude can be restricted either by Ohmic losses in resonator walls (in a long pulse or continuous wave operation) or by microwave breakdown in a short pulse operation.

Therefore, an alternative concept of high-power relativistic gyroamplifiers may be of interest, namely gyrotwistrons. For these devices with a traveling-wave output section, we have considered some basic features of interaction between traveling waves and relativistic electrons gyrating in a strongly tapered external magnetic field. We supplemented this consideration with the example showing very good agreement between optimal magnetic field tapering found in simulations and experimentally for the case of operation rather far from cutoff.

A further increase in the interaction efficiency of relativistic gyroamplifiers can be provided, first, by producing electron beams with low velocity spread and second, by utilizing high current electron beams in gyrotwistrons. The effect of increasing the current is to shorten the optimal interaction length which makes operation of the device less sensitive to velocity spread. However, to produce high current electron beams of a good quality is a major challenge for developers of electron guns.

[1] R. Q. Twiss, *Aust. J. Phys.* **11**, 567 (1958).
 [2] J. Schneider, *Phys. Rev. Lett.* **2**, 504 (1959).
 [3] R. H. Pantell, *Proc. IRE* **47**, 1146 (1959).
 [4] A. V. Gaponov, *Izv. Vyssh. Uchebn. Zaved. Radiofiz.* **2**, 450 (1959); **2**, 836 (1959).
 [5] J. L. Hirschfield and V. L. Granatstein, *IEEE Trans. Microwave Theory Tech.* **MTT-25**, 522 (1977).
 [6] E. S. Weibel, *Phys. Rev. Lett.* **2**, 83 (1959).
 [7] A. V. Gaponov, *Zh. Eksp. Teor. Fiz.* **39**, 326 (1960) [Sov. Phys. JETP **12**, 232 (1960)].
 [8] A. V. Gaponov and V. K. Yulpatov, *Radiotekh. Elektron.* **12**, 627 (1967) [Radio Eng. Electron. Phys. **12**, 582 (1967)].
 [9] K. R. Chu and J. L. Hirshfield, *Phys. Fluids* **21**, 461 (1978).
 [10] A. A. Kolomenskii and A. N. Lebedev, *Dokl. Akad. Nauk. SSSR* **145**, 1259 (1962) [Sov. Phys. Dokl. **7**, 745 (1963)].
 [11] V. Ya. Davydovskii, *Zh. Eksp. Teor. Fiz.* **43**, 886 (1962) [Sov. Phys. JETP **16**, 629 (1963)].
 [12] V. A. Flyagin and G. S. Nusinovich, *Proc. IEEE* **76**, 644 (1988).
 [13] A. V. Gaponov, A. L. Gol'denberg, M. I. Petelin, and V. K. Yulpatov, Copyright 223931 with priority of 24.03.1967. Official Bulletin, Komitet po Delam Izobreteni i Otkrytiy, Soviet Ministrov USSR, No. 11,200 (1976).
 [14] V. A. Flyagin, A. V. Gaponov, M. I. Petelin, and V. K. Yulpatov, *IEEE Trans. Microwave Theory Tech.* **MTT-25**, 514 (1977).
 [15] V. V. Alikaev, G. A. Bobrovskij, M. M. Ofitserov, V. I. Poznyak, and K. A. Razumova, *Pis'ma Zh. Eksp. Teor. Fiz.* **15**, 41 (1972) [JETP Lett. **15**, 27 (1972)].
 [16] K. E. Kreischer and R. J. Temkin, *Infrared and Millimeter Waves* (Academic, New York, 1983), Vol. 7, p. 377.
 [17] V. A. Flyagin, A. L. Gol'denberg, and G. S. Nusinovich, *Infrared and Millimeter Waves* (Academic, New York, 1984), Vol. 11, p. 179.
 [18] V. L. Bratman, N. S. Ginzburg, and G. S. Nusinovich, *Pis'ma Zh. Tekh. Fiz.* **3**, 961 (1977) [Soviet Tech. Phys. Lett. **3**, 395 (1977)].
 [19] M. I. Petelin, *Izv. Vyssh. Uchebn. Zaved. Radiofiz.* **17**, 902 (1974) [Sov. Radiophys. **17**, 686 (1974)].
 [20] V. L. Bratman, N. S. Ginzburg, G. S. Nusinovich, M. I. Petelin, and P. S. Strelkov, *Int. J. Electron.* **51**, 541 (1981).
 [21] V. L. Bratman and G. G. Denisov, *Int. J. Electron.* **72**, 969 (1992).
 [22] K. D. Pendergast, B. G. Danly, W. L. Menninger, and R. J. Temkin, *Int. J. Electron.* **72**, 983 (1992).
 [23] N. S. Ginzburg, *Izv. Vyssh. Uchebn. Zaved. Radiofiz.* **30**, 1181 (1987) [Sov. Radiophys. **30**, 865 (1987)].
 [24] G. S. Nusinovich, *Phys. Fluids B* **4**, 1989 (1992).
 [25] V. L. Bratman, N. S. Ginzburg, and A. V. Savilov, in

High-Frequency Relativistic Electronics, edited by A. V. Gaponov-Grekhov (Inst. Appl. Phys., Nizhny Novgorod, Russia, 1992), Issue 7, p. 22.

[26] W. Lawson, J. P. Calame, B. Hogan, P. E. Latham, M. E. Read, V. L. Granatstein, M. Reiser, and C. D. Striffler, *Phys. Rev. Lett.* **67**, 520 (1991).

[27] P. E. Latham, W. Lawson, and V. Irwin, *IEEE Trans. Plasma Sci.* **PS-22**, 804 (1994).

[28] K. R. Chu, V. L. Granatstein, P. E. Latham, W. Lawson, and C. D. Striffler, *IEEE Trans. Plasma Sci.* **PS-13**, 424 (1985).

[29] W. Lawson and P. E. Latham, *IEEE Trans. Microwave Theory Tech.* **40**, 1973 (1992).

[30] N. S. Ginzburg, I. G. Zarnitsyna, and G. S. Nusinovich, *Izv. Vyssh. Uchebn. Zaved. Radiofiz.* **24**, 481 (1981) [Sov. Radiophys. **24**, 331 (1981)].

[31] V. L. Ginzburg and I. M. Frank, *Dokl. Akad. Nauk SSSR* **56**, 583 (1947).

[32] V. L. Bratman and A. E. Tokarev, *Izv. Vyssh. Uchebn. Zaved. Radiofiz.* **17**, 1224 (1974) [Radiophys. Quantum Electron. **17**, 932 (1974)].

[33] N. S. Ginzburg, *Izv. Vyssh. Uchebn. Zaved. Radiofiz.* **22**, 470 (1979) [Radiophys. Quantum Electron. **22**, 323 (1979)].

[34] J. L. Vomvoridis, *IEEE Trans. Nucl. Sci.* **NS-20**, 3124 (1983).

[35] T. H. Kho and A. T. Lin, *Phys. Rev. A* **38**, 2883 (1988).

[36] V. A. Zhurakhovsky, *Nonlinear Oscillations of Electrons in Magnetically Confined Beams* (Naukova Dumka, Kiev, 1972) (in Russian).

[37] C. S. Roberts and S. J. Buchsbaum, *Phys. Rev. A* **135**, 381 (1964).

[38] A. V. Gaponov, M. I. Petelin, and V. K. Yulpatov, *Izv. Vyssh. Uchebn. Zaved. Radiofiz.* **10**, 1414 (1967) [Radiophys. Quantum Electron. **10**, 794 (1967)].

[39] A. F. Kurin, *Radiotekh. Elektron.* **34**, 616 (1990) [Radio Eng. Electron. Phys. (USSR) **34** (8), 115 (1991)].

[40] Y. Gell, J. R. Torstensson, H. Wilhelmsson, and B. Levush, *Appl. Phys. B* **27**, 15 (1982).

[41] W. Lawson and W. W. Destler, *IEEE Trans. Plasma Phys.* **PS-22**, 895 (1994).

[42] R. S. Symons and H. R. Jory, in *Advances in Electrons and Electron Physics*, edited by L. Marton (Academic, New York, 1981), Vol. 55, p. 1.

[43] G. S. Nusinovich and O. Dumbrajs, *Phys. Plasmas* **2**, 568 (1995).

[44] S. N. Vlasov, G. M. Zhislin, I. M. Orlova, M. I. Petelin, and G. G. Rogacheva, *Izv. Vyssh. Uchebn. Zaved. Radiofiz.* **12**, 1236 (1969) [Radiophys. Quantum Electron. **12**, 972 (1969)].

[45] M. I. Petelin and V. K. Yulpatov, *Izv. Vyssh. Uchebn. Zaved. Radiofiz.* **18**, 290 (1975) [Radiophys. Quantum Electron. **18**, 212 (1975)].

[46] G. S. Nusinovich and H. Li, *Phys. Fluids B* **4**, 1058 (1992).

[47] Ya. L. Bogomolov, V. L. Bratman, and N. S. Ginzburg, *Fiz. Plazmy* **13**, 1399 (1987) [Sov. J. Plasma Phys. **13**, 810 (1987)].

[48] A. T. Lin, W. W. Chang, and C. C. Lin, *Phys. Fluids* **27**, 1054 (1984).

[49] K. D. Pendergast, B. G. Danly, R. J. Temkin, and J. S. Wurtele, *IEEE Trans. Plasma Sci.* **16**, 122 (1988).

[50] J. K. Lee, W. D. Bard, S. C. Chiu, R. C. Davidson, and R. R. Goforth, *Phys. Fluids* **31**, 1824 (1988).

[51] P. E. Latham, W. Lawson, V. Irwin, B. Hogan, G. S. Nusinovich, H. W. Matthews, and M. K. E. Flaherty, *Phys. Rev. Lett.* **72**, 3730 (1994).

[52] P. E. Latham and G. S. Nusinovich, in *Advanced Accelerator Concepts, Port Jefferson, NY, 1992*, edited by J. S. Wurtele, AIP Conf. Proc. No. 279 (AIP, New York, 1993), p. 42.

[53] A. W. Fliflet, *Int. J. Electron.* **61**, 1049 (1986).

[54] G. S. Nusinovich and H. Li, *Int. J. Electron.* **72**, 895 (1992).

[55] N. S. Ginzburg, A. S. Sergeev, and A. V. Smorgonsky, *Zh. Tekh. Fiz.* **59**, 135 (1989) [Sov. Phys. Tech. Phys. **34**, 332 (1989)].

[56] A. K. Ganguly and S. Ahn, *Phys. Rev. A* **42**, 3544 (1990).